Gold nanoparticle-initiated free radical oxidations and halogen abstractions

Petre Ionita, Marco Conte, Bruce C. Gilbert and Victor Chechik*

Received 30th July 2007, Accepted 7th September 2007
First published as an Advance Article on the web 20th September 2007
DOI: 10.1039/b711573c

We report on the use of EPR spectroscopy and spin trapping technique to detect free radical intermediates formed in the presence of gold nanoparticles. Phosphine- and amine-protected gold nanoparticles were found to initiate air oxidation of organic substrates containing active hydrogen atoms, such as amines and phosphine oxides. Nanoparticles protected by stronger bound ligands (*e.g.*, thiols) were inactive in these reactions. We also found that gold nanoparticles are able to abstract a halogen atom from the halogenated compounds, presumably due to the high affinity of gold metal for halogens. Reaction of Au nanoparticles with chloroform showed an unusual inverse isotope effect. The trichloromethyl spin adduct was observed when Au nanoparticles were mixed with $CDCl_3$ but not with $CHCl_3$. This unexpected behaviour suggests that C–H bond breaking is not the rate-determining step in Au-initiated hydrogen abstraction.

Introduction

Gold nanoparticles are an example of simple-to-make, well-defined nanostructures, which can be used for a variety of applications.[1] One area where gold particles are attracting much interest is catalysis. Since the early reports on the remarkable activity of supported Au nanoparticles in CO oxidation,[2] many other reactions catalysed by Au nanoparticles showed unusual activity and/or selectivity.[3] Recent reports on the high activity of homogeneous Au catalysts in such reactions as oxidations, reductions, alkene additions, cycloisomerisations *etc.*, further expand the scope of potential applications of Au nanoparticle catalysts.[4] Au catalysis thus became one of the fastest developing areas in homogeneous and heterogeneous catalysis alike.[5]

Despite the advances in Au nanoparticle catalysis, the mechanistic features of these reactions remain largely unexplored. Some metal-catalysed reactions (*e.g.*, oxidations and reductions) are likely to proceed *via* formation of free radical intermediates. Such reactions are best studied by EPR spectroscopy and spin trapping methods. For instance, hydrogen spillover on supported Pd catalysts was investigated in late 1990s by Mile and Maher *et al*.[6] Although this work clearly demonstrated the potential of EPR spectroscopy in uncovering the subtle details of the mechanisms of the nanoparticle-catalysed reactions, there have been virtually no further reports in this area, as highlighted in a recent review.[7]

During our study of the ligand exchange reactions on the surface of Au nanoparticles, we discovered that some of these processes occur *via* a free radical mechanism.[8] We detected formation of sulfur-centred radicals in an exchange reaction between triphenylphosphine-protected gold nanoparticles and an alkanethiol. The formation of S-centred radicals was probably due to the oxidation of thiol by molecular oxygen in the presence of the gold nanoparticles.[8,9] The proposed mechanism involved the adsorption of the oxygen on the nanoparticle surface as a superoxide species. Other compounds, such as hydroperoxides or hydrides were also oxidised under the same conditions.[8]

Similar catalytic properties of Au nanoparticles have been observed by Meisel *et al.*[9] Exposure of amino-TEMPO to atmospheric oxygen in the presence of Au nanoparticles led to the formation of oxo-TEMPO (Fig. 1). The authors suggested a mechanism which involved electron transfer from the amino group to oxygen, with the formation of a hydroperoxide radical, leading finally to the removal of the amino group and its replacement with a ketone group.

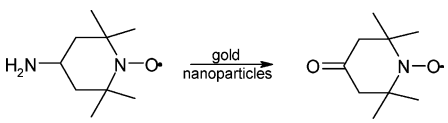

Fig. 1 Oxidation of amino-TEMPO by gold nanoparticles.[9]

In order to ascertain if formation of such free radical intermediates is a general feature of the Au nanoparticle-catalysed reactions, we used spin trapping and EPR spectroscopy to probe other related systems. Here, we report the results of this study. The spin adducts were obtained using DMPO and PBN spin traps (Fig. 2).

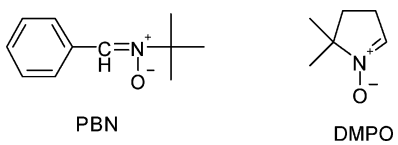

Fig. 2 Chemical structures of the PBN and DMPO spin-traps.

Results and discussion

Oxidation of amines and phosphine oxides by gold nanoparticles

The properties of gold nanoparticles depend on their size and on the nature or protecting ligands; the latter also determine their solubility. We have screened a series of different types

Department of Chemistry, University of York, Heslington, York, UK YO10 5DD. E-mail: vc4@york.ac.uk; Fax: (+44)-1904-432516

of nanoparticles for the ability to generate free radicals in the presence of air and organic substrates such as thiols or amines. The protecting ligands tried included triphenylphosphine (1.4 nm),[10] butanethiol (2.5 nm),[11] tetraoctylammonium bromide (4.7 nm),[12] citrate/chloride ions (13 nm),[13] dodecylamine (3.0 nm).[14]

The substrates used in this work were *n*-butylamine [as we were interested to see if Au-catalysed oxidation of amino-TEMPO[9] (*vide supra*) can be extended to other systems], and diphenylphosphine oxide. Both substrates contain reactive hydrogen attached to a heteroatom which could be abstracted by a peroxide-type species.

We found that only Au nanoparticles protected by triphenylphosphine and (to a lesser extent) alkylamines were able to initiate oxidation reactions. This was also confirmed using other organic substrates which were reported in the previous study (*e.g.*, *n*-butanethiol, borohydride, *t*-butyl hydroperoxide).[8] The lack of activity of the thiol-protected particles can be partially explained by poisoning of the reactive surface with thiolate ligands. The inactivity of the relatively large citrate-based nanoparticles is probably due to the small surface area and low nanoparticle concentration. Low solubility of oxygen in water can also explain the failure to detect any free radical intermediates in reactions in water (which were carried out in the presence of citrate-stabilised particles).

Triphenylphosphine-protected nanoparticles, in the reaction with butylamine in the presence of air and DMPO as a spin-trap, led to the corresponding N-centred spin-adduct of DMPO, well evidenced in the EPR spectrum (Fig. 3). The N-centred radical, assigned as $C_4H_9NH\cdot$, was also observed with the PBN spin trap. Reaction of dodecylamine-protected Au nanoparticles with butylamine in the presence of air and a spin trap (DMPO or PBN) also showed the presence of N-centred radicals; however, the intensity of the EPR peaks of the spin adducts in this case was lower. The assignment of EPR spectra was achieved by comparing the spectra with the genuine spin-adduct formed by oxidation of the corresponding amine with lead dioxide or hydrazyl radicals.[8,15]

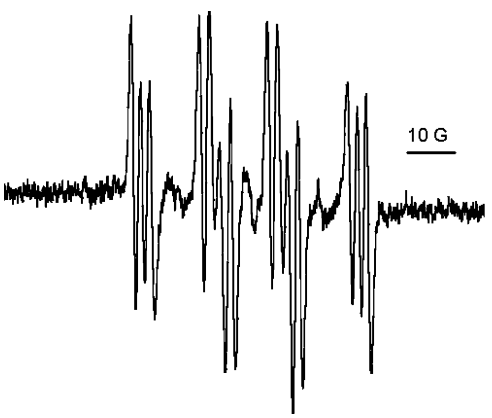

Fig. 3 EPR spectrum of the C_4H_9NH–DMPO spin adduct in toluene.

In order to optimise the spin trapping process and observe the highest concentration of the spin adduct, different parameters were varied, such as absolute and relative concentration of reactants, and reaction time. It was found that in all cases the formation of the spin adduct was very fast (<1 min), and increasing the reaction time did not lead to any increase in the amount of spin adducts (as judged by the EPR intensity). The addition of more amine after the formation of the spin-adduct also did not increase the intensity of the EPR spectra of the spin adduct.

In the reaction of diphenylphosphine oxide with phosphine- or amine-protected nanoparticles in the presence of DMPO or PBN, a signal corresponding to the P-spin adduct was observed. The radical was assigned as $Ph_2PO\cdot$.[16] The spectrum assignment was confirmed by comparison with a spectrum of an authentic $Ph_2PO\cdot$ radical obtained by oxidation of diphenylphosphine oxide with either lead dioxide or hydrazyl radicals. Deoxygenation of the reaction mixture prior to the addition of the spin traps led to significant reduction of the EPR intensity, further confirming that the oxidation requires the presence of molecular oxygen (Scheme 1).

$$R_2X\text{-}H \xrightarrow{Au,\ O_2} R_2X\cdot \xrightarrow{DMPO} R_2X\text{-}DMPO$$

Scheme 1 Au nanoparticle-initiated oxidation of organic compounds.

Interestingly, the half-life time of the $Ph_2PO\cdot$ spin adduct prepared by the nanoparticle-initiated reaction was much shorter (<1 min) than that of the same spin adduct prepared by oxidation with lead dioxide (up to 1 h). This difference in the lifetime can only be explained by the presence of gold nanoparticles. To confirm this, we have added triphenylphosphine-protected Au nanoparticles to the solution of a $Ph_2PO\cdot$–DMPO spin-adduct which was prepared by oxidation of the corresponding substrate with lead dioxide. A rapid disappearance of the EPR signal was indeed observed. In the case of a PBN spin-adduct prepared in the same way, the influence of the addition of the gold nanoparticles was almost unnoticeable.

Rapid disappearance of the DMPO spin-adduct in the presence of Au nanoparticles is likely to be due to a further reaction on the Au surface, or possibly a reaction with an Au(I) or Au(III) species. Au(III) in particular is a strong oxidising agent and is known to oxidise the spin-traps DMPO and PBN to form persistent free radicals.[17] Au(I) compounds are often considered possible intermediates in the ligand exchange reaction on the Au nanoparticle surface; hence we cannot exclude the presence of small amounts of Au(I) either in solution or on the Au surface. We must stress, however, that we observed no free radical intermediates in control experiments when Au nanoparticles were replaced by Au(I) or Au(III) compounds.

Halogen abstraction

We noticed that in some halogenated solvents, triphenylphosphine-protected gold nanoparticles were particularly unstable, aggregating and precipitating within one or two days. In order to check if this behaviour is accompanied by formation of any radical intermediates, we added spin traps (*e.g.*, DMPO and PBN) to toluene containing halogenated solvents, such as chloroform, dichloromethane, carbon tetrachloride, bromobutane, iodomethane, and chlorobenzene. In all cases except chlorobenzene and dichloromethane, very strong EPR signals of different spin-adducts were observed. PBN and DMPO spin traps captured the same radicals in all reaction mixtures. Dodecylamine-protected Au nanoparticles also gave the same results. Unlike nanoparticle-initiated oxidation reactions (*vide supra*), the halogen abstraction reaction does not depend on the presence of oxygen in the reaction mixture, as shown by carrying out spin trapping under a nitrogen

atmosphere. Fig. 4 shows the EPR spectra of the DMPO spin adducts with $\cdot CHCl_2$ and $\cdot CCl_3$.

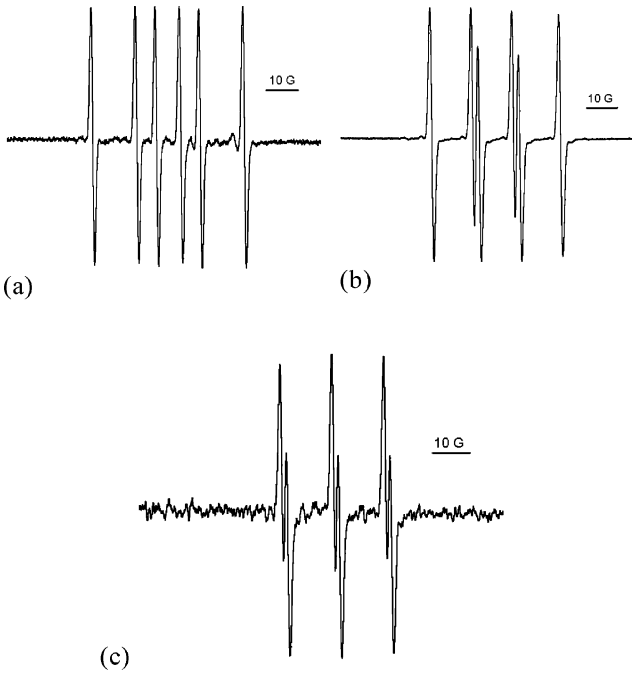

Fig. 4 EPR spectrum of the DMPO–$CHCl_2$ spin adduct prepared by abstraction of a Cl atom from chloroform (a), DMPO–CCl_3 spin adduct prepared by abstraction of a Br atom from $BrCCl_3$(b), and PBN–CCl_3 spin adduct formed by the same reaction (c).

The EPR parameters of the spin adducts formed are shown in Table 1. The assignment (with the exception of DMPO–$CDCl_2$) was carried out by comparison with the literature values. Although the a_N values for all C-centred radicals are very similar, the a_H values showed large variation even for the PBN adducts which enabled unambiguous assignment. The DMPO–$CDCl_2$ spin adduct has not been reported in the literature, and we have not been able to generate the $\cdot CDCl_2$ radical by alternative reactions; nonetheless, the hyperfine parameters strongly support the assignment, and the PBN spin adduct of this radical gave a perfect match with the literature parameters. Besides, formation of the $\cdot CDCl_2$ radical by halogen abstraction parallels similar reactions for CCl_4, $BrCCl_3$, CH_3I, C_4H_9Br.

Table 1 Hyperfine splitting constants for the DMPO and PBN spin-adducts obtained using triphenylphosphine-protected Au nanoparticles. Values in brackets are literature data

Substrate	Radical	Spin trap	a_N/G	a_H/G	a_X/G
$C_4H_9NH_2$	$C_4H_9NH\cdot$	DMPO	13.89	16.49	1.79 (a_N)
		PBN	14.11	2.10	—
Ph_2PHO	$Ph_2PO\cdot$	DMPO	13.86	18.18	37.71 (a_p)
		PBN	14.20	3.09	18.73 (a_p)
CCl_4	$\cdot CCl_3$	DMPO	13.10	15.16	—
			(13.17)[18]	(15.28)[18]	—
		PBN	13.91	1.54	—
			(13.60)[19]	(1.86)[19]	—
$CHCl_3$	$\cdot CHCl_2$	DMPO	13.66	19.76	—
		PBN	14.41	2.12	—
			(14.32)[19]	(3.03)[19]	—
$CDCl_3$	$\cdot CCl_3$	DMPO	13.30	15.62	—
	$\cdot CDCl_2$		13.65	19.77	—
	$\cdot CDCl_2$	PBN	14.39	2.08	—
CH_3I	$\cdot CH_3$	DMPO	14.27	20.61	—
			(14.20)[20]	(20.80)[20]	—
		PBN	14.80	3.56	—
			(14.94)[21]	(3.63)[21]	—
$CBrCl_3$	$\cdot CCl_3$	DMPO	13.14	15.17	—
		PBN	13.95	1.52	—
C_4H_9Br	$\cdot C_4H_9$	DMPO	14.17	22.34	—
		PBN	14.83	3.62	—
			(14.57)[21]	(3.22)[21]	—

The mechanism of halogen abstraction by the Au nanoparticles could be explained by electron transfer from the nanoparticle to the alkyl halide to create a radical anion which would then release halide anion and form a carbon-centred radical. The Au nanoparticle in this mechanism would become positively charged. Stepwise charging of Au nanoparticles by electrochemical reduction–oxidation is well known and thus support the feasibility of this mechanism.[22] Alternatively, the radicals can be formed by a direct attack of Au nanoparticles on the alkyl halide leading to the transfer of halogen atom (Scheme 2). This mechanism (driven by the very high affinity of halogens for gold)[23] would lead to the formation of AuCl on the nanoparticle surface and possibly displacement of the original ligand (*e.g.*, triphenylphosphine). Halogen adsorption on the nanoparticle surface then results in particle aggregation (Scheme 2). This behaviour would explain the poor stability of triphenylphosphine-stabilised Au nanoparticles in some chlorinated solvents (*e.g.*, CCl_4). Although unambiguous mechanistic conclusion is not possible, direct halogen abstraction seems more likely.

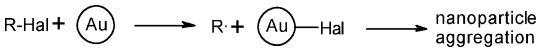

Scheme 2 Abstraction of halogen (Hal) atoms by Au nanoparticles.

Although spin-trapping data unambiguously show that radical intermediates are formed in the Au nanoparticle-initiated reactions, it is conceivable that these radicals are adsorbed on the nanoparticle surface and do not exist as free species in solution. For instance, spin adducts have been observed for some transition metal-catalysed reactions, even though the reaction stereochemistry ruled out formation of free radical intermediates. This was tentatively explained by the group transfer between the spin trap and the transition metal complex, which results in the formation of the spin adduct.[24] A similar process can be envisaged for Au nanoparticle-initiated reaction (Scheme 3).

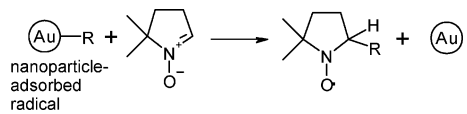

Scheme 3 Possible formation of spin adducts *via* formation of nanoparticle-adsorbed radicals.

In order to test this possibility, we explored competitive trapping of the $C_4H_9S\cdot$, $C_4H_9NH\cdot$ and $\cdot PPh_2O$ radicals by a 1 : 1 mixture of DMPO and PBN spin traps (Fig. 5). The same radicals were generated using either of the two oxidants: diphenyl picryl hydrazyl (DPPH), or Au nanoparticles in air. The radicals were then trapped by the mixture of spin traps, and the ratios of the PBN–DMPO spin adducts were calculated by simulating the experimental spectra as

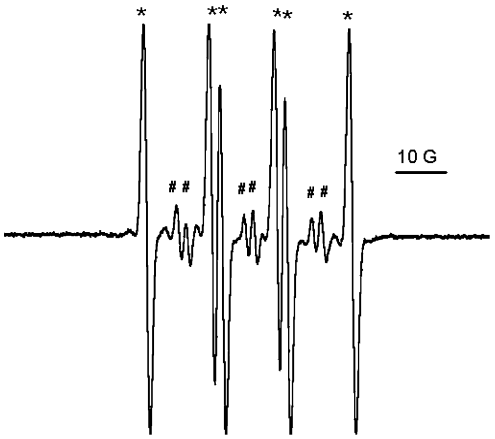

Fig. 5 EPR spectrum obtained using an equimolecular mixture of DMPO and PBN shows a mixture of DMPO–CCl_3 (*) and PBN–CCl_3 (#) spin adducts.

a mixture of two components. The logic behind this experiment was that DPPH-generated radicals definitely exist as free species in solution. If nanoparticle-generated radicals are also free species, one would expect to see exactly the same ratio of DMPO–PBN spin adducts for DPPH and nanoparticle-generated radicals. If the nanoparticle-generated radicals are adsorbed on the nanoparticle surface, the ratio could be different.

The results of this competitive trapping are shown in Table 2. It is worth noting that the selectivity of trapping depends strongly on the nature of the radical. However, DMPO is a much better substrate for the majority of radicals, and the DMPO spin adducts were the predominant species in most cases.

For the N-, P- and S-centred radicals generated using Au nanoparticles, we did not observe any PBN spin adduct. On the other hand, PBN adducts were observed if the same radicals were generated using DPPH (Table 2). Unfortunately, the stability of the $\cdot PPh_2O$ spin adducts is very limited in the presence of Au nanoparticles, and the kinetics of the spin adduct decay are quite complex and poorly reproducible. Therefore, even the observed large differences between the DMPO–PBN spin adduct ratios for DPPH and Au nanoparticle-generated radicals could in principle be explained by the instability of the spin adducts. On the other hand, the DMPO and PBN adducts of the nitrogen-centred radical were quite stable in the presence of Au nanoparticles. The slightly different (but readily observed in the EPR spectra) DMPO–PBN selectivity for this radical generated by reaction with Au particles or DPPH (Table 2) therefore supports the interactions of the free nitrogen-centred radicals with the nanoparticle surface (Scheme 3).

Table 2 Relative percentage of DMPO spin adduct in competitive binding of radicals with a mixture of DMPO–PBN spin traps. The data in brackets refer to DPPH-generated radicals; all other data refer to the radicals generated using triphenylphosphine-protected gold nanoparticles

Substrate	Percentage of DMPO spin adduct (%)
$C_4H_9NH_2$	100 (98.8)
Ph_2PHO	100 (39.4)
C_4H_9SH	100 (100)
CCl_4	98.5
$CHCl_3$	87.7
$CDCl_3$	39.1[a]/52.8[b]
CH_3I	81.9
$CBrCl_3$	95.4

[a] For $\cdot CCl_3$ spin-adduct. [b] For $\cdot CDCl_2$ spin adduct.

Interestingly, reactions of Au nanoparticles with chloroform and deuteriated chloroform gave unexpected results. DMPO spin trapping in a mixture of Au nanoparticles with chloroform (either neat or in toluene solution) gave the $\cdot CHCl_2$ adduct as the only EPR-active product. However, the same reaction with $CDCl_3$ showed *simultaneous* formation of $\cdot CCl_3$ and $\cdot CDCl_2$ spin adducts, with a ratio close to 1, as estimated by the simulation of the experimental spectra (Fig. 6).

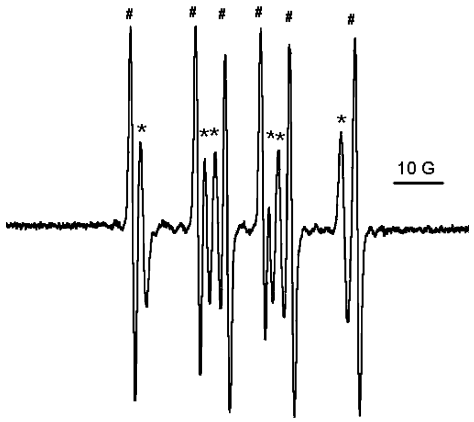

Fig. 6 EPR spectrum obtained from reaction of triphenylphosphine-protected Au nanoparticles and $CDCl_3$ in air. The observed spectra were identified as a mixture of DMPO–CCl_3 (*) and DMPO–$CDCl_2$ (#) spin adducts.

This result is difficult to explain. Formation of the $\cdot CCl_3$ radical (which is unambiguously assigned by comparison with the literature values and authentic species generated from CCl_4 and $CBrCl_3$) can only be explained by the abstraction of the H atom from $CHCl_3$. This reaction (if it involves breaking of the C–H bond in the rate-determining step) must exhibit a primary isotope effect, *e.g.*, it should be much faster for $CHCl_3$ than for $CDCl_3$. However, we only observed $\cdot CCl_3$ radical in the reaction of $CDCl_3$, not with $CHCl_3$. If the formation of $\cdot CCl_3$ radical does not involve breaking of the C–H/C–D bond in the rate-determining step, it should exhibit secondary isotope effects (which can be either normal or inverse); however, secondary isotope effects are usually small (*e.g.*, $0.5 < k_H/k_D < 2$) and hence cannot explain complete absence of the $\cdot CCl_3$ radical in the $CHCl_3$–Au nanoparticles reaction mixture.

We have carefully considered the possibility of artefacts. The absence of the CCl_3–DMPO adduct could be explained by a contamination in $CHCl_3$ (*e.g.*, stabiliser). This was ruled out by thoroughly purifying chloroform according to published protocols.[25] Additionally, a 1 : 1 mixture of $CHCl_3$ and $CDCl_3$ showed the presence of $\cdot CCl_3$ radical in the concentration, consistent with the amount of $CDCl_3$ used, thus further confirming the absence of reactive impurities in $CHCl_3$.

Another artefact could be caused by the formation of $\cdot CCl_3$ radical from an impurity in $CDCl_3$ which cannot be efficiently removed by purification (*e.g.*, $BrCCl_3$ or CCl_4). For instance, we found that the efficiency of the formation of $\cdot CCl_3$ adduct from

$BrCCl_3$ is extremely high. In order to check if the formation of radicals can be linked to the presence of impurities, we performed the following control experiment. Two samples of the same batch of $CHCl_3$ were treated with H_2O–NaOH and D_2O–NaOH under the same reaction conditions to obtain the samples of $CHCl_3$ and $CDCl_3$ with the same "handling history".[26] The formation of $CDCl_3$ was monitored by ^{13}C NMR. However, reaction of Au nanoparticles with these two solvents (in the presence of DMPO) confirmed that $CHCl_3$ gives only $\cdot CHCl_2$ radical while $CDCl_3$ gives a mixture of $\cdot CCl_3$ and $\cdot CDCl_2$. This apparent inverse isotope effect is hence a genuine phenomenon which cannot be explained by the presence of impurities. Our results thus strongly suggest that C–H bond breaking is not the rate-determining step in the overall hydrogen atom abstraction mechanism.

Conclusions

Triphenylphosphine-protected Au nanoparticles can activate molecular oxygen, and the reactive species formed are capable of abstracting a hydrogen atom from many organic molecules including alkylamines and diarylphosphine oxides. The structure of the free radicals thus formed was confirmed using EPR spectroscopy and spin-trapping technique. Alkylamine-protected Au nanoparticles are less active in the same reactions.

Reaction of phosphine or amine-protected Au nanoparticles with compounds possessing an active halogen atom (*e.g.*, alkyl bromides/iodides, chloroform, tetrachloromethane) led to the abstraction of the halogen atom by the Au nanoparticles. The radicals thus formed were also identified using spin trapping. The results of the competitive trapping using a mixture of two spin traps suggest interactions between the alkylamine-derived radical intermediate with the Au surface.

Interactions of chloroform with Au nanoparticles showed unexpected inverse isotope effect. The $\cdot CCl_3$ radical (presumably formed by abstraction of a hydrogen atom from chloroform) was observed in $CDCl_3$ but not in $CHCl_3$. This suggests that breaking of the C–H bond is not the rate-determining step of the hydrogen abstraction.

Experimental section

EPR spectra were recorded at room temperature in deoxygenated toluene, using a Jeol JES-RE1X spectrometer. The typical settings for the EPR spectra were: frequency 9.42 GHz, power 1 mW, sweep width 100 G, centre field 3190 G, sweep time 60 s, time constant 30 ms, modulation frequency 100 kHz, modulation width 1 G, gain 200. The spectra simulation was carried out using WinSim software.[27]

DMPO, PBN and other chemicals were purchased from Aldrich and used without further purification, except chloroform which was purified as described in ref. 24. The butanethiol-,[11] tetraoctylammonium bromide,[12] citrate-,[13] and dodecylamine-protected Au nanoparticles[14] were prepared following literature recipes. The butanethiol-protected nanoparticles were additionally purified by gel permeation chromatography using BioBeads SX-1 gel and dichloromethane as an eluent. Other nanoparticles were purified as described in the literature recipes.

Triphenylphosphine-protected Au nanoparticles[10] were prepared as follows. A 1% aqueous hydrogen tetrachloroaurate trihydrate solution (10 mL) was added to a toluene solution (10 mL) of tetraoctylammonium bromide (160 mg) and stirred for 5 minutes. When the gold layer had transferred to the organic phase, triphenylphosphine (230 mg) was added under stirring. After 2 min, a freshly prepared aqueous solution (5 mL) of $NaBH_4$ (140 mg) was rapidly added. The organic phase immediately turned dark brown. The reaction mixture was stirred for 3 h. The toluene layer was separated and the solvent was removed under vacuum at 40 °C to give a dark brown solid. The solid was redissolved in the minimum amount of dichloromethane and purified by gel permeation chromatography using Bio-Beads SX-1 as a stationary phase and dichloromethane as an eluent.

The spin trapping was performed as follows: the appropriate spin trap (0.1 mL of 0.1 M solution in toluene) was added to the substrate (0.1 mL of 0.1 M solution in toluene for non-halogenated substrates, or 0.1 mL of neat halogenated solvent). The resultant mixture was then added to a solution of gold nanoparticles in toluene (0.2 mL 2×10^{-4} M). The mixture was transferred into a glass tube and deoxygenated by bubbling nitrogen for *ca.* 1 min prior to recording the EPR spectra. All experiments were carried out at room temperature. The competitive spin trapping was carried out in the same way using a 1 : 1 equimolar ratio of DMPO–PBN. The spin trapping with DPPH and lead dioxide was also used in the same way using a 0.1 mL solution of DPPH in toluene (1 mM.) or *ca.* 50 mg of solid PbO_2.

$CDCl_3$ was prepared by the following procedure.[26] $CHCl_3$ (5 mL) was mixed with a 1 M NaOH solution in D_2O (15 mL) at 35 °C under a N_2 atmosphere and the mixture was stirred vigorously for 1.5 h. In order to increase the yield of the deuteration, the product was again treated with NaOH in D_2O for 1.5 h at 35 °C to obtain 90% isotope purity. $CHCl_3$ was prepared by an identical procedure using H_2O rather than D_2O.

Acknowledgements

The authors would like to thank the EPSRC for funding (grants GR/S45300/01 and EP/E001629/1).

Notes and references

1 M. C. Daniel and D. Astruc, *Chem. Rev.*, 2004, **104**, 293.
2 M. Haruta and M. Date, *Appl. Catal., A*, 2001, **222**, 427.
3 X. Deng, B. K. Min, A. Guloy and C. M. Friend, *J. Am. Chem. Soc.*, 2005, **127**, 9267; M. D. Hughes, Y.-J. Xu, P. Jenkins, P. McMorn, P. Landon, D. I. Enache, A. F. Carley, G. A. Attard, G. J. Hutchings, F. King, E. H. Stitt, P. Johnston, K. Griffin and C. J. Kiely, *Nature*, 2005, **437**, 1132; J. Chou and E. W. McFarland, *Chem. Commun.*, 2004, 1648.
4 D. Astruc, F. Lu and J. Aranzaez, *Angew. Chem., Int. Ed.*, 2005, **44**, 78; X. Deng and C. M. Friend, *J. Am. Chem. Soc.*, 2005, **127**, 17178; A. Gupta, C. Rhim, C. Oh, R. Mane and S. Han, *Green Chem.*, 2006, **8**, 25; X. Zhang, H. Shi and B. Xu, *Angew. Chem., Int. Ed.*, 2005, **44**, 7132; A. S. K. Hashmi, *Gold Bull.*, 2003, **36**, 3; X. Yao and C.-J. Li, *J. Am. Chem. Soc.*, 2004, **126**, 6884.
5 A. S. K. Hashmi, *Angew. Chem., Int. Ed.*, 2005, **44**, 6990; M. Haruta, *Gold Bull.*, 2004, **37**, 27.
6 A. Burt, M. Emery, J. Maher and B. Mile, *Magn. Reson. Chem.*, 2001, **39**, 85; A. F. Carley, H. A. Edwards, B. Mile, M. W. Roberts, C. C. Rowlands, F. E. Hancock and S. D. Jackson, *J. Chem. Soc., Faraday Trans.*, 1994, **90**, 3341; A. F. Carley, H. A. Edwards, B. Mile, M. W. Roberts, C. C. Rowlands, S. D. Jackson and F. E. Hancock, *J. Chem. Soc.*, 1994, 1407.

7 B. Mile, *Curr. Org. Chem.*, 2000, **4**, 55.
8 P. Ionita, B. C. Gilbert and V. Chechik, *Angew. Chem., Int. Ed.*, 2005, **44**, 3720.
9 Z. Y. Zhang, A. Berg, H. Levanon, R. W. Fessenden and D. Meisel, *J. Am. Chem. Soc.*, 2003, **125**, 7959.
10 W. W. Weare, S. M. Reed, M. G. Warner and J. E. Hutchinson, *J. Am. Chem. Soc.*, 2000, **122**, 12890.
11 M. Brust, M. Walker, D. Bethell, D. J. Schiffrin and R. J. Whyman, *J. Chem. Soc., Chem. Commun.*, 1994, 801.
12 J. Fink, C. J. Kiely, D. Bethell and D. J. Schiffrin, *Chem. Mater.*, 1998, **10**, 922.
13 J. Turkevich, P. C. Stevenson and J. Hiller, *Discuss. Faraday Soc.*, 1951, **11**, 55.
14 D. V. Leff, L. Brandt and J. R. Heath, *Langmuir*, 1996, **12**, 4723.
15 P. Ionita, B. C. Gilbert and A. C. Whitwood, *Lett. Org. Chem.*, 2004, **1**, 70.
16 We originally used diphenyl phosphine PPh_2H as a substrate and assigned the trapped radical as $\cdot PPh_2$. The reviewer suggested that due to fast oxidation of secondary phosphines, the trapped radical may be $\cdot PPh_2O$. Control experiments confirmed this suggestion, as PbO_2 oxidation of both PPh_2H and PPh_2HO gave the same spin adduct, and use of PPh_2O as a substrate in experiments with Au nanoparticles produced the same results as PPh_2H. ^{31}P NMR showed that solutions of PPh_2H rapidly oxidise toform PPh_2HO under ambient conditions. We thank the reviewer for correcting our initial error.
17 A. Nakajima, Y. Ueda, N. Endoh, K. Tajima and K. Makino, *Can. J. Chem.*, 2005, **83**, 1178.
18 D. L. Haire, U. M. Oehler, P. H. Krygsman and E. G. Janzen, *J. Org. Chem.*, 1988, **53**, 4535.
19 M. J. Davies and T. F. Slater, *Chem.-Biol. Interact.*, 1986, **58**, 137.
20 P. J. Barker, S. R. Stobart and P. R. West, *J. Chem. Soc., Perkin Trans. 2*, 1986, 127.
21 E. G. Janzen, U. M. Oehler, D. L. Haire and Y. Kotake, *J. Am. Chem. Soc.*, 1986, **108**, 6858.
22 R. Guo, D. Georganopoulou, S. W. Feldberg, R. Donkers and R. W. Murray, *Anal. Chem.*, 2005, **77**, 2662.
23 H.-S. Oh, J. H. Yang, C. K. Costello, Y. M. Wang, S. R. Bare, H. H. Kung and M. C. Kung, *J. Catal.*, 2002, **210**, 375.
24 J. F. Peyronel and H. B. Kagan, *New J. Chem.*, 1978, **2**, 211; J. K. Stille and K. S. Y. Lau, *Acc. Chem. Res.*, 1977, **10**, 434.
25 W. L. Armarego, D. D. Perrin, *Purification of laboratory chemicals*, Butterworth-Heinemann, Oxford, 4th edn, 1997.
26 E. A. Symons and J. D. Bonnett, *J. Catal.*, 1985, **93**, 209.
27 http://epr.niehs.nih.gov/pest.html.